IEEE Access
Multidisciplinary | Rapid Review | Open Access Journal

Received April 22, 2021, accepted May 7, 2021, date of publication May 14, 2021, date of current version May 25, 2021.

Digital Object Identifier 10.1109/ACCESS.2021.3080299

Workspace Design and Trajectory Planning of a Five Degree of Freedom Mobile Welding Manipulator for Spherical Objects

TAIMOOR ZAHID[1], ZAREENA KAUSAR[2], MUHAMMAD FAIZAN SHAH[3], MUHAMMAD TALLAL SAEED[2,4], AND JIANFEI PAN[1], (Member, IEEE)

[1]College of Mechatronics and Control Engineering, Shenzhen University, Shenzhen 518060, China
[2]Department of Mechatronics Engineering, Air University, Islamabad 44000, Pakistan
[3]Department of Mechanical Engineering, Khawaja Fareed University of Engineering & IT, Rahim Yar Khan 64200, Pakistan
[4]Department of Intelligent Systems and Control Engineering, School of Automation Sciences and Electrical Engineering, Beihang University, Beijing 100083, China

Corresponding author: Jianfei Pan (pan_jian_fei@163.com)

This work was supported in part by the Natural Science Foundation of China under Grant U1913214, and in part by the China Postdoctoral Foundation under Grant 2019M653038.

ABSTRACT Mobile Manipulators (MM) has attracted a lot of researchers for incorporation in the robotics field owning to their multitude of applications in real world. Welding automation has its wide applications in industry like automobile manufacturing and power generation industry involving spherical tanks. The objective of this study is to design workspace and devise a methodology to plan position trajectory of welding tool that produces smooth welding while the mobile platform turns simultaneously. The robot proposed in this paper has the manipulator mounted on a platform moving as a turntable to increase the workspace and enhances the mobility of the manipulator. The earlier produces linear segment of weld while the later produces parabolic segment. The kinematic equations for mobile platform and the mounted manipulator are described in detail. The workspace of the robot is visualized based on computations of transformation matrices and jacobians structured based on kinematic equation. Trajectories for each joint, computed using inverse kinematic equations, are also presented. For spherical trajectories the solution of system equations is combined with constraint values for each manipulator joint, thus allowing computation of desired joint position at any time interval. The efficacy of the proposed methodology for the trajectory planning is tested through a case study. The simulation results of motion transformation, workspace and trajectory show that linear segments of the trajectory combine with parabolic trajectory segments smoothly with zero acceleration within designed reachable workspace. The experimental results verify the efficacy of application of presented kinematic and inverse kinematic models for welding of spherical objects.

INDEX TERMS Degrees of freedom, kinematics, mobile manipulator, trajectory, welding workspace.

I. INTRODUCTION

Since last few years welding manipulators are being extensively studied by the researchers [1]–[10]. One of the main benefits of welding manipulators apart from the working conditions and production efficiency is that these manipulators can be used for small scale processes, especially in mechanical fields such as metal component sewing, manufacture and other industrial applications [11]. Currently, research is mainly focused on the design and control systems for welding robots, mainly in intelligent control systems [12] and adaptive control systems [13]. The need for mobile robotic welding has increased in today's industrial environments. One of the areas is the manufacturing of storage tanks that are spherical or cylindrical in shape. Most of the welding process is conducted manually and there is shortage of expertise in seam welding on spherical objects. In order to improve quality of weld seam and to overcome shortage of expertise in welding of spherical tanks, automatic welding equipment is needed. Recent development in robotics field has led to automatic welding operations. One of these emerging trends is the mobile welding. In this paper we propose a mobile manipulator that is capable

The associate editor coordinating the review of this manuscript and approving it for publication was Yingxiang Liu.

of welding tasks on spherical or cylindrical objects getting a motivation from a problem of turning of welding vehicle and positioning of welding torch in autonomous mobile welding robot. Such welding robots, however, need devising a method to find the kinematic variables ensuring that the required welding function in the spherical objects is satisfied.

Recent work on such mobile robots for welding applications has been done by Kim *et al.* [14] and Jeon *et al.* [15]. These manipulators are developed for three dimensional laser vision systems for the welding of ship and seam tracking, respectively. A mobile welding robot for straight welding path with sensors is proposed by Kam *et al.* [16]. A mobile robot using a sliding mode control for tracking a smooth curved path is proposed by Chung *et al.* [17]. Tang has proposed a mobile welding robot for large steel structures in industries [18]. Pan proposes a welding manipulator based on screw theory [19]. Cuong proposes a mobile welding manipulator for horizontal fillet joints [20].

For such mobile manipulators, it is necessary to analyze its kinematic solutions and trajectory from design till experimental phase [21], [22]. Kinematic solutions for such robots are quite complex because of link constraints [11]. Much research is being carried out to solve these problems [23]. Researchers [24]–[26] have presented intelligent mobile robots for welding on spherical tanks where the robot base is fixed on tank surface and the manipulator travels on the spherical surface. A welding mobile manipulator may combine a moving platform and a robotic manipulator to increase mobility and dexterous space of the robot for use in an automated manufacturing environment. A study on the mobile manipulators for welding in ship building industry is carried out for the Lattice type structure [27]. The mobile welding manipulator for spheres, in literature, has a three linked manipulator mounted on a two wheeled platform but it can operate in a straight path [28] only. The motion planning on spherical surface is presented in [29]. However, mobility of the manipulator is desired to be explored and that needs to model the mobile robotic manipulator for control of the wheeled mobile robotic manipulators [30]–[34].

The importance of developing a mobile welding manipulator is effectively realized for hazardous environments where human presence is hazardous. The commercial robots suffer from disadvantage of lack of mobility since they are fixed at one designated place. Besides, a fixed manipulator has a limited range of motion. Most of the welding operations performed are manually suffered from inaccurate welding seam due to inaccurate welding speed and position [35]. To our knowledge, autonomous mobile robots are in existence, however, extensive work has yet to be conducted in mobile manipulators for welding operations. The main purpose of this paper is not only to enhance the manipulator workspace by mounting it on a mobile platform but to produce smooth welding while the mobile platform turns simultaneously, proves to be challenging on curved spherical paths.

In the paper, a wheeled mobile manipulator configuration has been proposed following a concept of rotating table to realize reliably moving of welding torch on the surface of spherical tank. The welding on spherical tanks require combination of linear and parabolic path segments. Therefore, a 4-DOF welding manipulator has been fixed on 1-DOF robotic platform to carry out the welding tasks on spheres. The manipulator and the mobile platform move simultaneously along the desired path. A methodology is devised to plan the desired path giving smooth weld. We present the mathematical model of the proposed mobile welding manipulator and the workspace is computed numerically. The Denavit-Hartenberg (DH) convention is followed to formulate the kinematic equations of the mobile welding manipulator. As the proposed welding manipulator is a 4 Degree of Freedom (DOF) manipulator with 1 DOF mobile platforms, So there are in total 5 DOF of the proposed configuration. In section II, the detailed description of the proposed manipulator is given. In section III, the kinematics of the manipulator is discussed. In section IV the differential motions of the proposed mobile welding manipulator are discussed. Section V presents the details about the workspace of the proposed mechanism. Section VI discusses the trajectory planning followed by results and discussions in section VII.

II. DESCRIPTION OF MOBILE WELDING MANIPULATOR

A design for the two-wheeled mobile welding manipulator for spherical objects should meet the criteria of mobility, spherical workspace and structure stability. The mobility is required to approach the seam to be weld. Spherical workspace is required to cover the entire spherical shape. Structural stability is required to maintain a certain range of shapes.

The mobile welding manipulator consists of four major components: a mobile base to give 1 DOF, a 4 DOF robotic arm, software algorithm to compute workspace and trajectory and the electric circuitry to implement computed motions. A model of the base and the arm of the mobile welding manipulator is developed using SolidWorks®.

The base of the welding manipulator is proposed to be made up of a rigid frame. Figure 1 shows the rigid base frame and the mobile welding manipulator. The material for the base of the robot is proposed to be aluminum which is a lightweight but strong material. The dimensions of the robot base are: length 40 cm, Width 40 cm and height is 20 cm. The base is propelled by differential drive wheels with a feedback sensor and controller.

The manipulator, a robotic arm, consists of three links and an end effector. The first link of the manipulator is capable of 360° rotations along the y-axis. The second and third links are capable of angular rotation of 180°. The end effector is fixed on the third link. Figure 1 shows the two-wheeled mobile robotic manipulator with base, designed for spherical objects.

There is 1 DOFs of the mobile platform, whereas 4 DOFs are fixed for the manipulator at top. The DOF can be obtained from the Chebychev Grubler-Kutzbach criterion as

$$DOF = \sigma\,(N - J - 1) + \sum_{i=1}^{J} F_i \qquad (1)$$

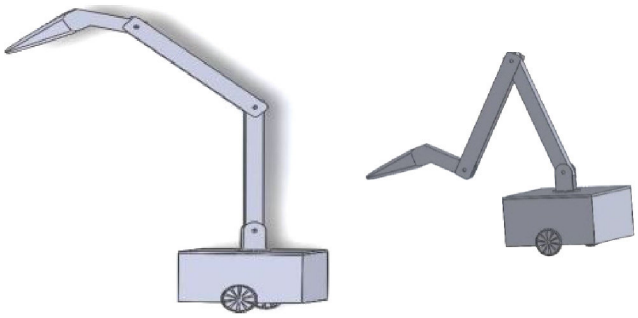

FIGURE 1. Proposed SolidWorks® model of the mobile welding manipulator.

where N is the total number of links including the fixed link (or base), J is the total number of joints connecting two consecutive links, F_i is the degrees of freedom at the i^{th} joint. The value of σ is 6 for motion in space and is 3 for planar motion.

III. KINEMATICS MODEL

Kinematics refers to the study of position, velocity and acceleration of the manipulator regardless of the force. Kinematics study can be categorized as forward kinematics and inverse kinematics. Forward kinematics involves the motion of the end effector of the manipulator in terms of link lengths and joint angles [36]. Inverse kinematics is computation of link lengths and joint parameters knowing the end effector position [37]. For the proposed mobile welding manipulator a comprehensive kinematics study is carried out as follows.

A. FORWARD KINEMATICS

The problem of kinematics is to deal with the position and orientation of the robot manipulator without considering the forces and torques that produce the motion. The proposed mobile welding manipulator is a 4 DOF manipulator without the mobile base. The motion transformation is defined in each frame $\{i\}$, relative to the previous frame $\{i-1\}$. This transform is a function of four link parameters. Each of these four transformations is a function of one link parameter only, and the other three parameters can be fixed by mechanical design.

The links of the manipulator are $a1, a2, a3, a4$. θ is the angle of rotation or variable in our equation of motion as follows;

$$T_i^{i-1} = \begin{pmatrix} c\theta_i & -s\theta_i & 0 & a_{i-1} \\ s\theta ca_{i-1} & c\theta_i ca_{i-1} & -sa_{i-1} & -sa_{i-1}d_i \\ s\theta_i sa_{i-1} & c\theta_i sa_{i-1} & ca_{i-1} & ca_{i-1}d_i \\ 0 & 0 & 0 & 1 \end{pmatrix} \quad (2)$$

In this research, forward kinematics problem is solved using DH representation technique. After the assignment of necessary frames, the DH table is filled by substituting the values in equation (2). The value of joints and links are determined from the schematic drawing of the manipulator shown in Figure 2.

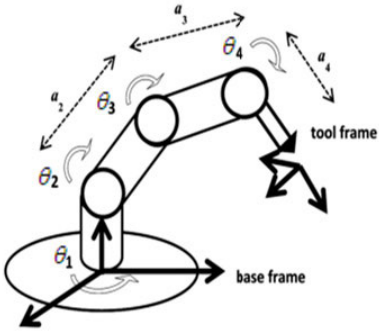

FIGURE 2. Schematic diagram of the proposed mobile welding manipulator.

The proposed mobile welding manipulator has two modeling components. Firstly, both the entities i.e. the manipulator and the mobile platform are modeled individually by assuming that during the movement of one body, the other entity remains static. In the second part, it is assumed that the mobile platform takes the manipulator to the desired target and the manipulator end effector is positioned to the seam to be weld. During the movement the mobile platform remains stationary. The DH representation of the manipulator links is given in the Table-1.

There are four revolute joints and each revolute joint offers one degree of freedom. Five frames are assigned to the manipulator. The homogenous transformations for formulation of forward kinematics of the fixed manipulator are given in equation (3),

$$T = {}_5^0T = {}_1^0T\,{}_2^1T\,{}_3^2T\,{}_4^3T\,{}_5^4T \quad (3)$$

Combining individual transformation equations following (3) results in (4):

$${}_5^0T = \begin{pmatrix} c\theta_1 c\theta_{234} & -c\theta_1 s\theta_{234} & s\theta_1 & P_x \\ s\theta_1 c\theta_{234} & -s\theta_1 s\theta_{234} & -c\theta_1 & P_y \\ s\theta_{234} & c\theta_{234} & 0 & P_z \\ 0 & 0 & 0 & 1 \end{pmatrix} \quad (4)$$

where p_x, p_y, p_z are the position equations of the manipulators in the three coordinates of this spatial serial 4 *DOF* manipulator and are calculated from equation (5) to (7), as shown at the bottom of the page.

$$P_x = c\theta_1[c\theta_2 c\theta_3(c\theta_4 l_4 + l_3 - s\theta_3(s\theta_4 l_4) - s\theta_2 s\theta_3(c\theta_4 l_4 + l_3) + c\theta_3(s\theta_4 l_4) = c\theta_1(c\theta_{234} l_4 + c\theta_{23} l_3 + c\theta_2 l_2) \quad (5)$$

$$P_y = s\theta_1[c\theta_2 c\theta_3(c\theta_4 l_4 + l_3 - s\theta_3(s\theta_4 l_4) + l_2 - s\theta_2 s\theta_3(c\theta_4 l_4 + l_3) + c\theta_3(s\theta_4 l_4) = s\theta_1(c\theta_{234} l_4 + c\theta_{23} l_3 + c\theta_2 l_2) \quad (6)$$

$$P_z = s\theta_2[c\theta_2 c\theta_3(c\theta_4 l_4 + l_3 - s\theta_3(s\theta_4 l_4) + l_2 + c\theta_2 s\theta_3(c\theta_4 l_4 + l_3) + c\theta_3(s\theta_4 l_4) + l_1 = s\theta_{234} l_4 + s\theta_{23} l_3 + s\theta_2 l_2 + l_1 \quad (7)$$

TABLE 1. Denavit-Hartenberg parameters.

i	α_{i-1}	a_{i-1}	d_i	θ_i
1	0	0	0	θ_1
2	9	0	$a1$	θ_2
3	0	$a2$	0	θ_3
4	0	$a3$	0	θ_4
5	0	$a4$	0	0

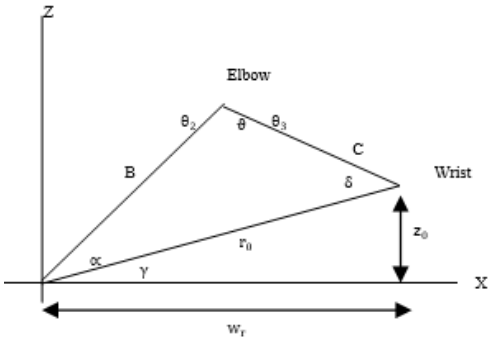

FIGURE 3. Side view of joints 2, 3 and 4.

B. INVERSE KINEMATICS

The inverse kinematics is used for deriving the joint values from the position coordinates. With inverse kinematics the value of each joint is determined to place the robot at a desired position and orientation. The equations that are derived for finding the joint angles are employed directly in robot programming to drive the robot to a desired position.

To move the robot along the desired trajectory the joint values of the robot are calculated many times. The robot was intended to follow a particular trajectory such a straight line or a curved line. There are different methods of calculating the inverse kinematics. The equations derived in the forward kinematics are highly non-linear transcendental equations. In case of serial manipulators up to 6 DOF the inverse kinematics of the manipulator is calculated through algebraic solutions, Geometric solutions or Numerical solutions. Geometric methods were used in this research to obtain the inverse kinematic model of the proposed mobile welding manipulator.

Geometrical parameters of the manipulator are shown in figure 2. The angle denoted by θ_1 is the angle through which the base of the robot, the moving platform, moves. The manipulator with the base of the robot at a standstill can rotate about the z-axis that passes through the joint axis. The 360^o rotation of the base increases the workspace of the welding manipulator and hence increased the object handling capability of the mobile manipulator around the robot body. The angle θ_1 can be calculated as (8).

$$\theta_1 = tan\left(\frac{y}{x}\right) \tag{8}$$

From figure 3 and figure 4, equations (9) and (10) can be obtained.

$$W_r = R - (D\ x\ cos\theta_4) \tag{9}$$

$$Z_o = (Z - (D\ x\ sin\theta_4)) - A \tag{10}$$

$$\gamma = atan\frac{(z_o)}{(W_r)} \tag{11}$$

By the geometric relation in figure 3,

$$r_o = \sqrt{z_o^2 + w_r^2} \tag{12}$$

By using the law of cosines in figure 3,

$$\propto = acos\left(\frac{r_0^2 + B^2 - C^2}{2 \times r_o \times B}\right) \tag{13}$$

and θ_2 is given as $\theta_2 = \alpha + \gamma$. From Figure 3 by law of cosines

$$\vartheta = acos\left(\frac{C^2 + B^2 - r_0^2}{2 \times C \times B}\right) \tag{14}$$

From Figure 3, θ_3 is given as $\theta_3 = (\theta_2 + \vartheta) - 180$.

C. KINEMATIC MODEL OF MOBILE MANIPULATOR

A schematic diagram of the mobile manipulator, combined wheeled base and the manipulator, is shown in Figure 5. In proposed mechanism, the two actuated wheels are supposed to be controlled by motors whereas the third passive wheel was for the stability of platform. The 4-link manipulator was mounted on top. Considering the mobile manipulator in figure 5 it was assumed that there is no lateral motion and the manipulator is mounted on the center of the platform.

Every joint is driven by an actuator. Joint 1, can move around z axis and the three links above joint 1 can rotate about z-axis. β represents the orientation of the mobile manipulator. The forward kinematics of the wheeled mobile manipulator, combined kinematics of the mobile platform and the manipulator, is derived in equations (15) and onwards in this section.

l_1, l_2, l_3, l_4 are link lengths. Similarly, $x_c = x + dcos\beta$ and $y_c = dsin\beta$. d is the distance between center of platform and center of axle of mobile base.

$$x_A = x_c + l_2 cos\theta_2 cos\,(\beta + \theta_1) + l_3 cos\,(\theta_2 + \theta_3)\,cos\,(\beta + \theta_1) + l_4 cos\,(\theta_3 + \theta_4)\,cos(\beta + \theta_1) \tag{15}$$

$$y_A = y_c + l_2 cos\theta_2 \sin\,(\beta + \theta_1) + l_3 \cos\,(\theta_2 + \theta_3) \sin\,(\beta + \theta_1) + l_4 \cos\,(\theta_3 + \theta_4) \sin(\beta + \theta_1) \tag{16}$$

$$z_A = l_1 + l_2 sin\theta_2 + l_3 sin\,(\theta_2 + \theta_3) + l_4 sin\,(\theta_3 + \theta_4) \tag{17}$$

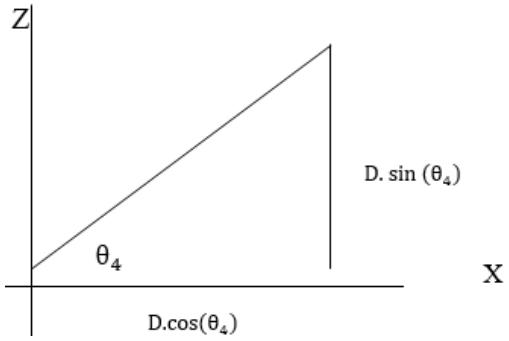

FIGURE 4. Side view of wrist joint.

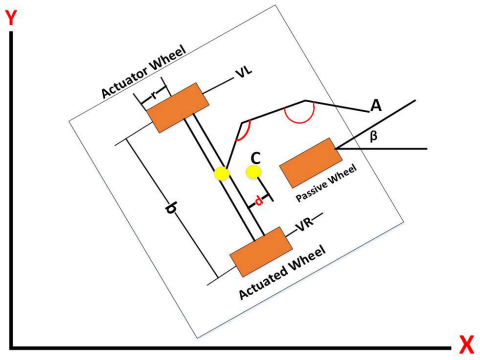

FIGURE 5. 2-D sketch of the mobile manipulator.

IV. DIFFERENTIAL MOTIONS OF THE MOBILE WELDING MANIPULATOR

In a seam welding task the robot joints need to move at a constant speed to maintain welding quality. The end-effector of the manipulator should move at a constant speed in a prescribed direction. The robot joint velocities were calculated and measured at any instance of time so that the total motion to be achieved at the end-effector of the robot. The movement at the end-effector of the manipulator is the resultant differential motion of the frame. Differential motion of a frame is divided as differential translations, differential rotations and a combination of different translations and rotations.

A differential translation is defined as the translation of the frame in differential amounts. A differential rotation is a small rotation of a frame if a frame rotates by an angle '$d\theta$' about any axes. The differential transformations are a combination of translations and rotations of a frame. We introduce a quantity as a differential operator Δ that is obtained as given in equation (18).

$$\Delta = (Trans * Rotation - Identity\ matrix) \tag{18}$$

In matrix form it can be represented as in equation (19).

$$\Delta = \begin{bmatrix} 0 & -\delta z & \delta y & dx \\ \delta z & 0 & -\delta x & dy \\ -\delta y & \delta x & 0 & dz \\ 0 & 0 & 0 & 0 \end{bmatrix} \tag{19}$$

The change in the differential frame dT from the frame T is given as in equation (20).

$$[dT] = [\Delta][T] \tag{20}$$

The matrix dT represents the change in frame after the differential motion. This matrix is given as in equation (21).

$$dT = \begin{bmatrix} dn_x & do_x & da_x & dp_x \\ dn_y & do_y & da_y & dp_y \\ dn_z & do_z & da_z & dp_z \\ 0 & 0 & 0 & 0 \end{bmatrix} \tag{21}$$

The new location and orientation of the frame after the differential motion can be found by adding the change in frame.

$$T_{new} = dT + T_{old} \tag{22}$$

The above equations give the changes made to a frame after the differential motion. The manipulator movements are translated into the change of frame at the end-effector and the frame changes result in the movement of the end effector of the frame. The differential motion and the Robot Jacobian in the end-effector frame are related to the joint movements of the manipulator. As the manipulator is a 4 degree of freedom robot, it is represented by equation (23).

$$\begin{bmatrix} d_x \\ d_y \\ d_z \\ \delta_x \end{bmatrix} = [Jacobian] \begin{bmatrix} d\theta_1 \\ d\theta_2 \\ d\theta_3 \\ d\theta_4 \end{bmatrix} \tag{23}$$

or

$$[D] = [J][D_\theta] \tag{24}$$

In the Homogenous transformation matrix given in equation (4), the first element p_x in last column of the matrix represents the motion of the end-effector along the x-axis, p_y represents the motion along y-axis and similarly p_z represents motion along z-axis, the derivatives of the corresponding elements are d_x, $d_y d_z$ respectively. The detailed calculations for the differential motions are explained in *Appendix*.

V. WORKSPACE

The mobile manipulator has the advantage of infinite workspace. However during the task execution, the mobile platform is standstill and the manipulator workspace is defined as the maximum allowable limits of the arm to reach the target. The reachable workspace describes the volume in space in which the manipulator end-effector can reach. The dexterous workspace is a subset of reachable workspace. The reachable workspace is defined by the motion of the end-effector and the related manipulator arms through their allowable limits.

By varying the degrees of freedom in the plane the end-effector can be positioned to occupy space within the reach of the manipulator. Singular configurations are given as $det\ (J(\theta)) = 0$. The determinant of the Jacobian is used to

measure manipulator dexterity. The manipulability measure 'w' is defined as $w = |det\ (J(\theta))|$

In order to have a smooth weld trajectory the manipulator revolute joints move at a constant velocity. To calculate joint velocities, we consider differential motions along the three axes. Jacobian calculations are required to find the revolute joints differential motions. Jacobians relates the joint differential motions to hand differential motions.

The inter-relationship between joint differential motions of a robot links to the differential motion of the hand frame is given as in equation (25).

$$\begin{bmatrix} d_x \\ d_y \\ d_z \\ \delta_x \end{bmatrix} = [J] \begin{bmatrix} d\theta_1 \\ d\theta_2 \\ d\theta_3 \\ d\theta_4 \end{bmatrix} \tag{25}$$

d_x, d_y, d_z represent differential motion in the x, y and z axis respectively. δ_x denotes the rotation around x-axis and $d\theta_1$ *to* $d\theta_4$ represent the differential motion of the joints. Jacobian is calculated relative to the last frame. The transformation matrix for the particular manipulator is given in (26).

$${}^0_5T = {}^0_1T^1_2T^2_3T^3_4T^4_5T = \begin{bmatrix} n_x & o_x & a_x & 0 \\ n_y & o_y & a_y & 0 \\ n_z & o_z & a_z & 0 \\ 0 & 0 & 0 & 1 \end{bmatrix} \tag{26}$$

$[J]$ matrix was calculated as given in equations (27) and (28).

$$J_{1i} = \left(-n_xP_y + n_YP_x\right); \quad J_{2i} = \left(-o_xP_Y + o_yP_x\right) \tag{27}$$

$$J_{3i} = \left(-a_xP_y + a_yP_x\right); \quad J_{4i} = n_z \tag{28}$$

To calculate the differential motions the joints of the manipulator the inverse Jacobian is needed as given by the $[D_\theta] = \left[J^{-1}\right][D]$.

VI. TRAJECTORY PLANNING

Using the inverse kinematics equations of the proposed mobile welding manipulator, the joint angles for the desired position and orientation are determined while the initial location and orientation of the mobile platform were known. The motion of each joint of the manipulator was planned individually. For the four degree of freedom manipulator under consideration the first joint angle of the robot was known for which the beginning of the motion segment at time t_i is θ_i and it was desired for the first joint to move to a new joint value θ_f at time t_f.

The constraints on the manipulator motion are the initial conditions and final conditions that are the initial velocities and accelerations which are known. The initial velocity of the first joint includes effects of the motion of the mobile platform which are assumed to be known. To produce smooth motion of end-effector in presence of simultaneous motion of mobile platform the velocity should be constant. An adaptive approach is proposed here giving three types of trajectories, presented here for different situations of the seam welding encountered on spheres. The trajectory of the robot is calculated and the four boundary conditions are known. The third order polynomial trajectory as given in equation (29).

$$\theta\ (t) = c_0 + c_1t + c_2t^2 + c_3t^3 \tag{29}$$

where the initial and final conditions are given in equations (30-a, b, c).

$$\Theta(t_i) = \theta_i \tag{30-a}$$

$$\theta\left(t_f\right) = \theta_f \tag{30-b}$$

$$\dot{\theta(t_i)} = 0$$

$$\dot{\theta(t_f)} = 0 \tag{30-c}$$

By taking the first derivative of the polynomial Equation (29),

$$\dot{\theta}\ (t) = c_1 + 2c_2t + 3c_3t^2 \tag{31}$$

Substituting the values of initial and final conditions in Equation (29) and (31),

$$\begin{bmatrix} \theta_i \\ \dot{\theta}_i \\ \theta_f \\ \dot{\theta}_f \end{bmatrix} = \begin{bmatrix} 1 & 0 & 0 & 0 \\ 0 & 1 & 0 & 0 \\ 1 & t_f & t_f^2 & t_f^3 \\ 0 & 1 & 2t_f & 3t_f^2 \end{bmatrix} \begin{bmatrix} c_0 \\ c_1 \\ c_2 \\ c_3 \end{bmatrix} \tag{32}$$

By solving the above linear system of equations and plugging the necessary constraint values the coefficients of the third order polynomial equation that allows to calculate the joint position at any interval of time can be calculated. The same process was repeated for the remaining joints.This third order polynomial of each joint creates a motion profile that was used to drive each manipulator joint.

Case Study: Assuming that in the mobile welding manipulator first joint is desired to go from an initial angle of 0° to final angle of 45° in 5 seconds. Substituting the boundary constraints in the Equation (32) yields;

$$\theta\ (t) = c_0 = 0° \tag{33-a}$$

$$\theta\left(t_f\right) = c_0 + c_1\ (5) + c_2\left(5^2\right) + c_3\left(5^3\right) = 45 \tag{33-b}$$

$$\dot{\theta}\ (t_i) = c_1 = 0 \tag{33-c}$$

$$\dot{\theta}\left(t_f\right) = c_1 + 2c_2\ (5) + 3c_3\left(5^2\right) = 0 \tag{33-d}$$

Solving the equations (33-a) to (33-d) yields;

$$c_0 = 0, \quad c_1 = 0,\ c_2 = 5.4,\ c_4 = -0.72$$

Substituting the desired time intervals in the position equation, motion of the first joint angle was calculated at the different time intervals.

A. FIFTH ORDER TRAJECTORY

There is a need to specify maximum accelerations at the initial and final points of movement. In order to specify velocities, positions and accelerations of the trajectory a fifth order polynomial was required, and six constants were needed.

$$\theta\ (t) = c_0 + c_1t + c_2t^2 + c_3t^3 + c_4t^4 + c_5t^5 \tag{34}$$

$$\dot{\theta}\ (t) = c_1 + 2c_2t + 3c_3t^2 + 4c_4t^3 + 5c_4t^4 \tag{35}$$

$$\ddot{\theta}\ (t) = 2c_2 + 6c_3t + 12c_3t^2 + 20c_3t^3 \tag{36}$$

B. LINEAR SEGMENT WITH PARABOLIC BLENDS

This type of trajectory is desired when a constant velocity is required for the manipulator as in case of welding it was desired that the velocity in linear and constant during the operation. So, at the start and end of the trajectory the constant ramping of the velocity profile is desired. The profile was divided into three segments. The linear segments were blended with parabolic blends at the beginning and end of the motion of the joint.

It is assumed that the initial and final positions are θ_i and θ_f at times $t_i = 0$ and t_f and parabolic segments are blended with the linear segments at times t_b and $t_f - t_b$; hence,

$$\theta(t) = c_0 + c_1 t + \frac{1}{2} c_2 t^2 \tag{37}$$

$$\dot{\theta}(t) = c_1 + c_2 t \tag{38}$$

$$\ddot{\theta}(t) = c_2 \tag{39}$$

In this scenario acceleration was constant at the parabolic segments. The first part of the segment from t_0 to t_b is a quadratic polynomial and at time t_b, blending time, the trajectory switches to a linear segment with constant velocity. At the third segment the trajectory profile switches to a linear section.

The common points where velocity is constant are called knot points. Substituting the boundary conditions into the parabolic equation segment yields,

$$\theta(t) = \theta_i + \frac{1}{2} c_2 t^2 \tag{40}$$

$$\dot{\theta}(t) = c_2 t \tag{41}$$

$$\ddot{\theta}(t) = c_2 \tag{42}$$

For the linear segment velocity was constant the initial velocity was zero and the linear segment has a constant velocity $\dot{\theta}$ and the final velocity at the end of motion was zero. The joint positions and velocities at two points and the final point were found as;

$$\theta_A = \theta_i + \frac{1}{2} c_2 t_b^2 \tag{43}$$

$$\dot{\theta}_A = c_2 t_b \tag{44}$$

$$\theta_B = \theta_A + \dot{\theta}(t_f - 2t_b) \tag{45}$$

$$\theta_f = \theta_B + (\theta_A - \theta_i) \tag{46}$$

$$\dot{\theta}_f = 0 \tag{47}$$

$$t_b = \frac{\theta_i - \theta_f + \dot{\theta} t_f}{\dot{\theta}} \tag{48}$$

The final parabolic segment was symmetrical and with the negative acceleration, it is shown as in equation (49).

$$\theta(t) = \theta_f - \frac{\dot{\theta}}{2t_b}(\dot{t}_f - t)^2 \tag{49}$$

$$\dot{\theta}(t) = \frac{\dot{\theta}}{t_b}(t_f - t) \tag{50}$$

$$\ddot{\boldsymbol{\theta}}(\boldsymbol{t}) = -\frac{\dot{\boldsymbol{\theta}}}{\boldsymbol{t_b}} \tag{51}$$

An adaptive approach is offered giving three methods which are presented to be used in three different constraints for simple to complex trajectories. The algorithm gives a choice depending on reference trajectory.

VII. RESULTS AND DISCUSSIONS

A. MOTION TRANSFORMATIONS OF THE MOBILE WELDING MANIPULATOR

The manipulator is required to achieve the Coordinates from $T1 = (0, 5, 0)$ to $T2 = (10, 15, 10)$. The transformation matrix was calculated in MATLAB software and the velocity, position and acceleration profiles were plotted against time. Angle profiles, velocity profiles and acceleration profiles for joints 1, 2, 3 and 4 can be seen in figures 6 to 11.

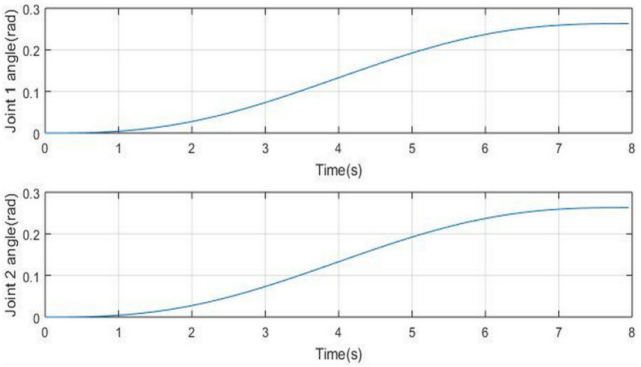

FIGURE 6. Angle profiles of joint 1 and 2.

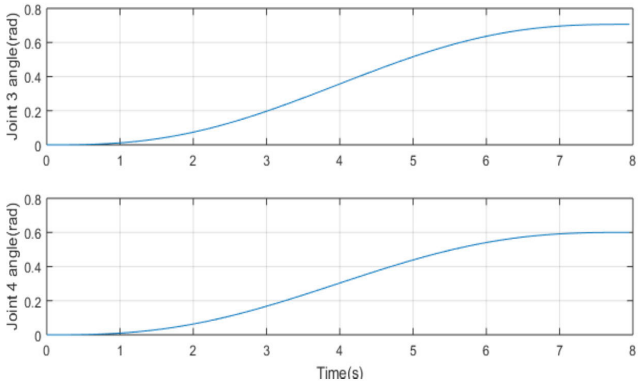

FIGURE 7. Angle profiles of joint 3 and 4.

Figure 12 is the model of the 4 DOF manipulator that is simulated using Peter Corke Matlab® toolbox in 3D coordinates.

B. WORKSPACE OF THE MOBILE WELDING MANIPULATOR

Various techniques have been adopted to determine the workspace for the manipulator. These techniques involve iterative and analytical techniques. A code was developed in this research using MATLAB® software to determine the

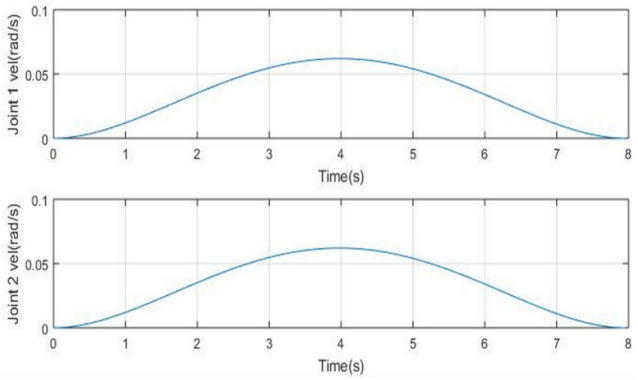

FIGURE 8. Velocity profiles of joint 1 and 2.

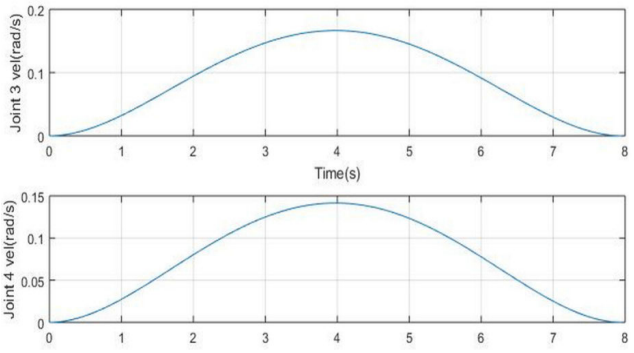

FIGURE 9. Velocity profiles of joint 3 and 4.

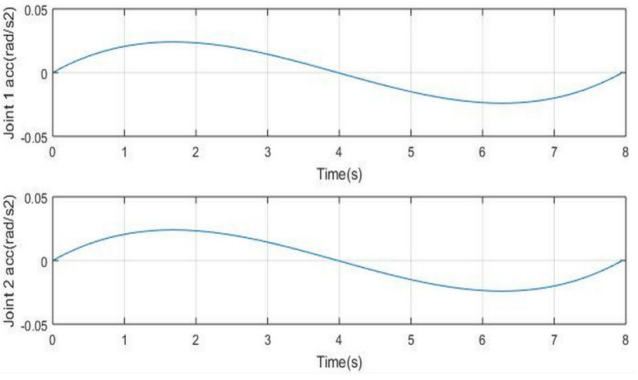

FIGURE 10. Acceleration profiles of joint 1 and 2.

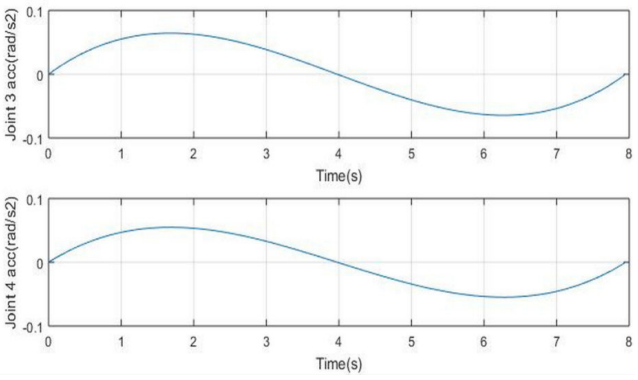

FIGURE 11. Acceleration profiles of joint 3 and 4.

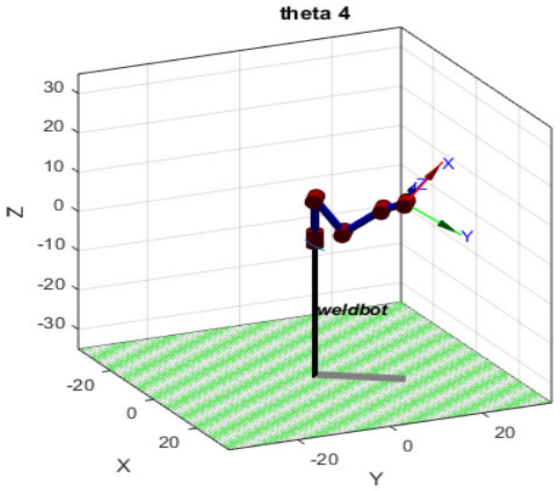

FIGURE 12. Peter cork model of the 4 DOF welding manipulator.

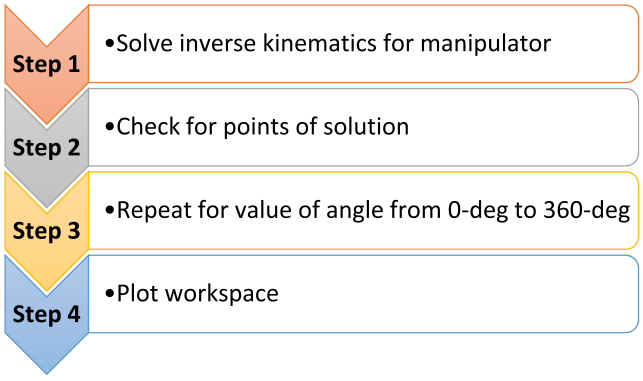

FIGURE 13. Algorithm for calculating the workspace of the welding manipulator.

workspace of the manipulator. Figure 13 shows the algorithm steps to obtain the workspace.

A point cloud that shows the limits based on selected link parameters and allowable degrees of rotation. The lengths of the arms l_1 to l_3 were fixed at 10 units and wrist arm l_4 at 5 units. The graphical view shows the joint extended reach and reachable area of the manipulator. Figure 14 (a) shows the point cloud of the workspace of the proposed manipulator.

As a case study three leg lengths l_2, l_3 and l_4 are selected to be 6, 5 and 3 cm respectively. Initial values of these three lengths were taken zero and the position points were plotted with step increment of 1 mm. l_2 is kept fixed. The values in the graph in figure 14 (b) shows the resulting reachable workspace of the manipulator.

The resulting workspace covers a whole sphere of a dimension. That means the proposed system is capable of approaching of any spherical shape depending on the lengths of the arms.

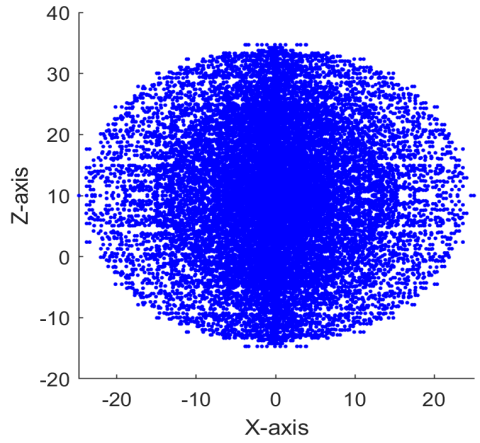

(a) Point Cloud of the Workspace of the Mobile Welding Manipulator

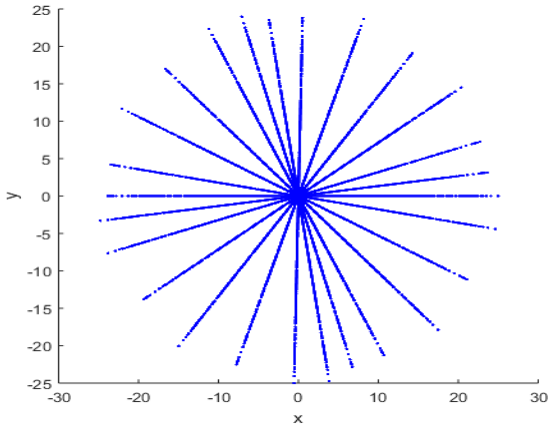

(b) Reachable Workspace of the Mobile Welding Manipulator

FIGURE 14. (a): Point cloud of the workspace of the mobile welding manipulator. (b): Reachable workspace of the mobile welding manipulator.

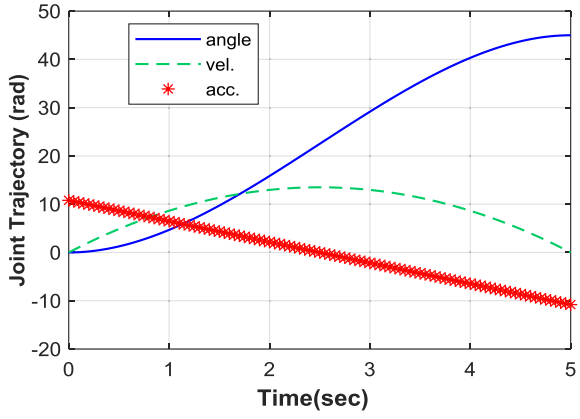

FIGURE 15. Trajectory profile using cubic polynomials.

C. TRAJECTORY PLANNING OF THE MOBILE WELDING MANIPULATOR

The trajectory generated for 1st revolute joint has physical limits from **0**° to **360**°. The trajectory is plotted as shown in figure 15. The position trajectory starts from **0**° all the way towards **45**°. As a constraint, the initial and final velocities of the system were zero.

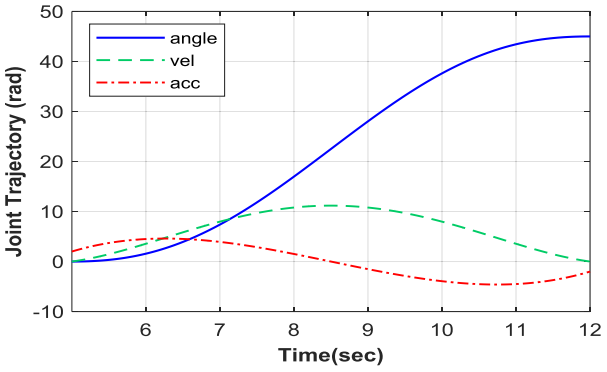

FIGURE 16. Trajectory profile using fifth order polynomials.

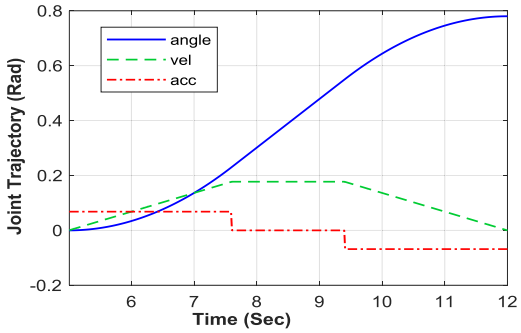

FIGURE 17. Trajectory profile using parabolic blends.

The fifth order trajectory polynomial is shown in figure 16. It is evident that the robot starts its movement from angle of 0 degrees. However, the specified initial and final accelerations we're starting from $\mathbf{2}^\circ/\boldsymbol{sec}^{\mathbf{2}}$ and ending at $-\mathbf{2}^\circ/\boldsymbol{sec}^{\mathbf{2}}$.

Linear segments with parabolic blends are simulated in MATLAB with the trajectory profile shown in figure 17. As it is evident from the above figure that the velocity of end effector is constant with the linear segment and the acceleration is zero, in presence of effects of simultaneous mobile platform motion, except for the starting and final velocity segments in which there is an increase and decrease in the velocity and corresponding result is shown as the acceleration and deceleration at the beginning and end of movement.

In the welding task it is required that the robot end- effector path to be planned more precisely for welding on a specific path. To move the manipulator end-effector on a straight path, there is requirement to specify the intermediate points or locations for the end-effector to pass through. These points should lie on the straight path connecting the starting and ending positions, these points are called the knot points.

D. EXPERIMENTAL SETUP

1) OPERATIONAL ALGORITHM

The manipulator works automatically. An algorithm designed to automate the manipulator operation is shown in figure 18 in the form of a flow diagram. The designed algorithm checks coordinates of the seam to be welded, calculate the joint

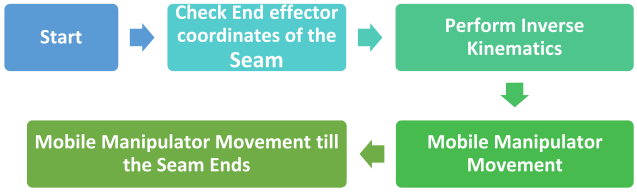

FIGURE 18. Flow chart for the working of the mobile welding manipulator.

angles of the arm and final position of wheels of base knowing a fixed speed of wheel motors. The algorithm gets feedback from position sensors, updates the torques required to approach to coordinates of the seam to be welded.

2) HARDWARE

In order to implement the algorithm, actuate and control the system four electronic devices are used: Adriano, Relays, IR sensors, and regulator. Relays are used to work with H-bridges to control the direction of wheel motors and joint motors. IR sensors are used to feedback position of wheels and path to follow. Wheels are to track the planned path. The power requirement is evaluated such that it requires voltage 12V and maximum current 7Ah. Use of the portable batteries to provide a designed power rating was preferred for the system.

The mobile platform is a four-wheel differential driven platform with two active powered wheels that are powered independently with dc motors and two passive caster wheels are attached to the mobile base for stability as the platform has to hold a manipulator therefore for stability of the platform caster wheels are attached. The mobile platform is required to travel/move in a curve around the spherical work piece. Wheeled mobile platform is steered with the two powered actuators such that two wheels can be steered individually. If one wheel turns in one direction and the other in the opposite direction, the robot can rotate at its position and any desired path can be achieved.

3) EXPERIMENTAL PROCEDURE

The fabricated model of the proposed mobile welding manipulator is tested to verify the reachable workspace and smooth weld of straight, curved, sinusoidal and complex infinity shaped seams on a spherical object as shown in figure 19a to 19d. Figures 19b to 19d clarifies the need of mobility and requirement of simultaneous motion of the manipulator and the mobile platform. The serial manipulator is unable to reach a workspace that covers perimeter of a spherical shape as shown in figures 19b-19d. This is shown with example of sinusoidal and infinity shaped trajectories on a sphere.

In figure 19b the fixed existing position of mobile platform is unable to draw the shapes completely on the sphere surface. With the change of position of mobile platform, however, the welding manipulator welded infinity shape completely as shown in figure 19c. Similarly, figure 19d shows desired results for a sinusoidal shape.

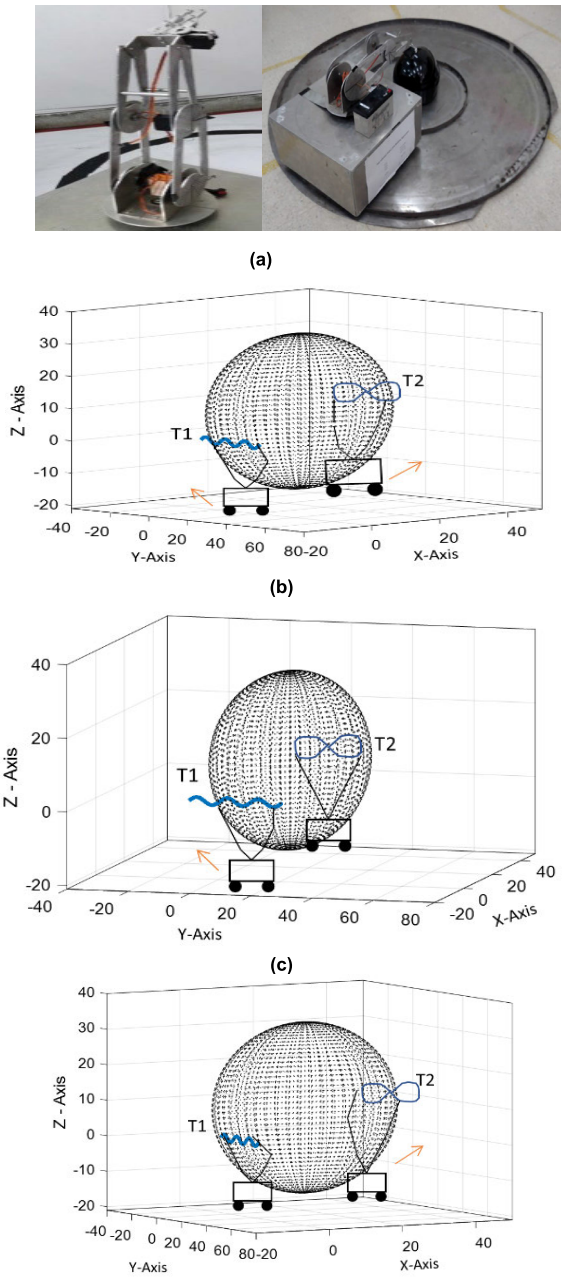

FIGURE 19. (a) Experimental setup of the 5 Degree of freedom welding manipulator during the testing for workspace analysis and motion profiles (b)-(d) an illustration of experimental procedure.

A set of coordinates for six seam trajectories is provided as input to the algorithm. The weld tool, end effector of the manipulator, moved to the given positions during these experiments at a velocity of 100mm/s on straight, sinusoidal, infinity shaped and curved line paths. The position and acceleration trajectories of the weld tool are measured and plotted as shown in figure 20.

4) EXPERIMENTAL RESULTS

It was observed that the manipulator is able to weld on the trajectory computed from the given set of points in the

TABLE 2. Maximum error in end-effector trajectories.

Trajectory type	*Straight*	*Slight curve*	*Half circle*	*Sinusoidal*	*Infinity shape*
Error (mm)	*0.5*	*1*	*1*	*1.5*	*1.5*

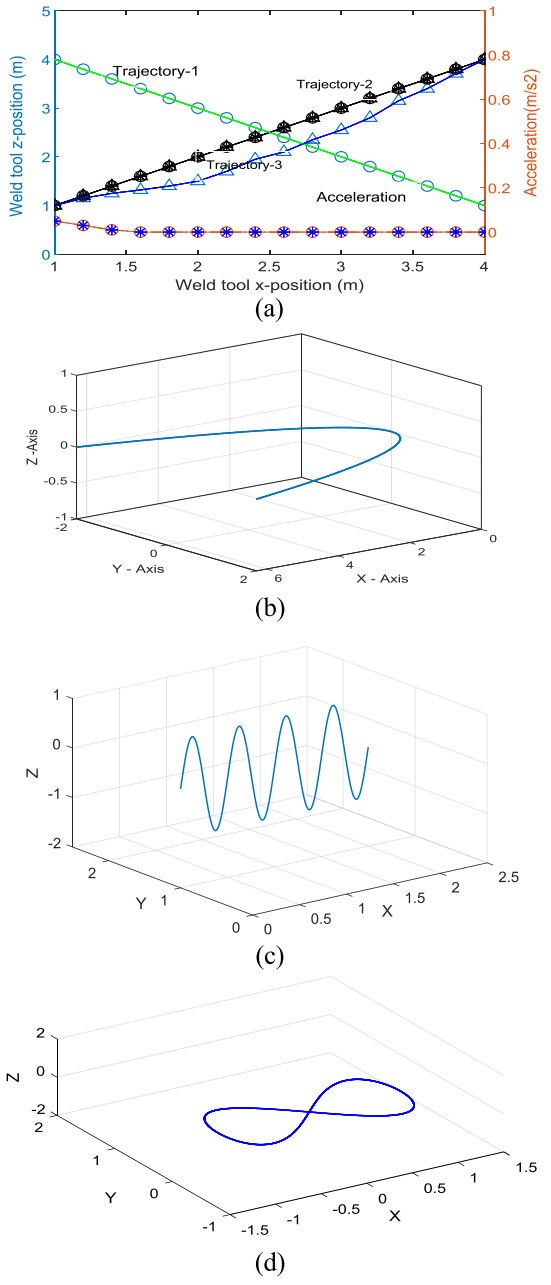

FIGURE 20. Experimental results (a) Three position trajectories including 2 straight and 1 slightly curved trajectory along with average acceleration. (b) Curved trajectory. (c) Sinusoidal trajectory. (d) Infinity shaped trajectory of weld seam.

spherical workspace as shown in figure 20. The results show that the algorithm is capable of producing trajectories within a spherical workspace. The paths planned and followed by the weld tool for the four seam trajectories are smooth, very small initially then zero acceleration. These results verify the efficacy of the proposed algorithm and models to be used for welding of spherical objects.

VIII. CONCLUSION

The two wheeled mobile manipulator is proposed with 5 degrees of freedom for welding of straight lines and curves on spherical tanks. The degrees of freedom of the mobile manipulator is constrained to minimum to achieve the desired welding task. The kinematics of the proposed mobile welding manipulator is analyzed in detail. The differential motions for the proposed mechanism are studied. Workspace of the mobile welding manipulator is studied along with the trajectory planning for the links of the proposed manipulator. The kinematic analysis results showed augmentation of the task space to spherical objects, whereas, the trajectory planning results produced smooth weld with simultaneous motion of the moving platform and manipulator. The dynamic analysis for torque minimization control and comparison of proposed path planning algorithm with complex algorithms such as given by [38], [39] are challenges to be studied in future.

APPENDIX

Jacobian is calculated relative to the last frame T^4, the velocity equation relative to the last frame is given by equation (A-1).

$$\left[D^{T_4}\right] = \left[J^{T_4}\right][D_\theta] \tag{A-1}$$

Homogeneous transformation matrix can be written as in (A-2).

$$\overset{R}{H}T = A_1A_2A_3A_4A_5 = \begin{bmatrix} n_x & o_x & a_x & 0 \\ n_y & o_y & a_y & 0 \\ n_z & o_z & a_z & 0 \\ 0 & 0 & 0 & 1 \end{bmatrix} \tag{A-2}$$

In order to have a smooth weld trajectory the manipulator revolute joints move at a constant velocity. To calculate joint velocities, we consider differential motions along the three axes. Jacobian calculations are required to find the revolute joints differential motions. Jacobians relates the joint differential motions to hand differential motions. All the joints under consideration are of revolute type so the corresponding elements of matrix in Homogeneous Transformations will be used to calculate the $[J]$ matrix.

$$J_{1i} = \left(-n_xP_y + n_YP_x\right); \quad J_{2i} = \left(-o_xP_Y + o_yP_x\right) \tag{A-3}$$

$$J_{3i} = \left(-a_xP_y + a_yP_x\right); \quad J_{4i} = n_z \tag{A-4}$$

To calculate the differential motions, the joints of the manipulator the inverse Jacobian are needed as given by the relation:

$$[D_\theta] = \left[J^{-1}\right][D] \tag{A-5}$$

To calculate the columns of the Jacobian matrix by using the convention:

$$\begin{aligned} {}^0_5T &= A_1A_2A_3A_4A_5 \\ {}^1_5T &= A_2A_3A_4A_5 \end{aligned}$$

$$
{}^{0}_{5}T = \begin{pmatrix} c\theta_1 c\theta_{234} & -c\theta_1 s\theta_{234} & s\theta_1 & c\theta_1[c\theta_2 c\theta_3(c\theta_4 l_4 + l_3 - s\theta_3\,(s\theta_4 l_4) + l_2 - s\theta_2 s\theta_3\,(c\theta_4 l_4 + l_3) + c\theta_3(s\theta_4 l_4) \\ s\theta_1 c\theta_{234} & -s\theta_1 s\theta_{234} & -c\theta_1 & s\theta_1[c\theta_2 c\theta_3(c\theta_4 l_4 + l_3 - s\theta_3\,(s\theta_4 l_4) + l_2 - s\theta_2 s\theta_3\,(c\theta_4 l_4 + l_3) + c\theta_3(s\theta_4 l_4) \\ s\theta_{234} & c\theta_{234} & 0 & s\theta_2[c\theta_2 c\theta_3(c\theta_4 l_4 + l_3 - s\theta_3\,(s\theta_4 l_4) + l_2 + c\theta_2 s\theta_3\,(c\theta_4 l_4 + l_3) + c\theta_3\,(s\theta_4 l_4) + l_1 \\ 0 & 0 & 0 & 1 \end{pmatrix} \tag{A-7}
$$

$$
{}^{0}_{5}T = \begin{pmatrix} c\theta_1 c\theta_{234} & -c\theta_1 s\theta_{234} & s\theta_1 & c\theta_1(C\,(\theta_2+\theta_3+\theta_4)\,l_4 + C\,(\theta_2+\theta_3)\,l_3 + C\theta_2 l_2) \\ s\theta_1 c\theta_{234} & -s\theta_1 s\theta_{234} & -c\theta_1 & s\theta_1((C\,(\theta_2+\theta_3+\theta_4)\,l_4 + C\,(\theta_2+\theta_3)\,l_3 + C\theta_2 l_2) \\ s\theta_{234} & c\theta_{234} & 0 & S\,(\theta_2+\theta_3+\theta_4)\,l_4 + S\,(\theta_2+\theta_3)\,l_3 + s\theta_2 l_2 + l_1 \\ 0 & 0 & 0 & 1 \end{pmatrix} \tag{A-8}
$$

$$
{}^{1}_{5}T = A_2 A_3 A_4 A_5 \tag{A-9}
$$

$$
{}^{1}_{5}T = \begin{pmatrix} c(\theta_2+\theta_3)c\theta_4 + s\theta_4 s(\theta_2+\theta_3) & -s\theta_4 c\,(\theta_2+\theta_3) + c\theta_4 s(\theta_2+\theta_3) & 0 & c\,(\theta_2+\theta_3)\,c\theta_4 l_4 + l_3 + s(\theta_2+\theta_3)\,(s\theta_4 l_4) + c\theta_2 l_2 \\ 0 & 0 & -1 & 0 \\ -s\theta_{23}c_4 - s_4 c(\theta_2+\theta_3) & -s4s\,(\theta_2+\theta_3) - c4c(\theta_2-\theta_3) & 0 & s\,(\theta_2+\theta_3)\,c\theta_4 l_4 + l_3 - c(\theta_2+\theta_3)\,(s\theta_4 l_4) + s\theta_2 l_2 + l_1 \\ 0 & 0 & 0 & 1 \end{pmatrix} \tag{A-10}
$$

$$
{}^{2}_{5}T = A_3 A_4 A_5 \tag{A-11}
$$

$$
{}^{2}_{5}T = \begin{pmatrix} c(\theta_3+\theta_4) & -s(\theta_3+\theta_4) & 0 & c_3\,(c_4 l_4 + l_3) - s_3 s_4 l_4 + l_2) \\ s(\theta_3+\theta_4) & c(\theta_3+\theta_4) & 0 & s_3\,(c_4 l_4 + l_3) + c_3 s_4 l_4 \\ 0 & 0 & 1 & 0 \\ 0 & 0 & 0 & 1 \end{pmatrix} \tag{A-12}
$$

$$
{}^{3}_{5}T = A_4 A_5 \tag{A-13}
$$

$$
{}^{3}_{5}T = \begin{pmatrix} c\theta_4 & -s\theta_4 & 0 & c\theta_4 l_4 + l_3 \\ s\theta_4 & c\theta_4 & 0 & s\theta_4 l_4 \\ 0 & 0 & 1 & 0 \\ 0 & 0 & 0 & 1 \end{pmatrix} \tag{A-14}
$$

$$
\begin{aligned} {}^{2}_{5}T &= A_3 A_4 A_5 \\ {}^{3}_{5}T &= A_4 A_5 \end{aligned} \tag{A-6}
$$

After putting the values of matrices in above equations will give us following relations

Simplifying (A-7) yields,

Similarly;

The Jacobian matrix elements are given as;

$$
{}^{T_5}_{11}J = \left(-n_x P_y + n_y p_x\right) = -[(s_1 c_{234}\,(c_1 c_{234})\,l_4 + c_{23} l_3 + c_2 l_2) + (s_1 c_{234}\,(c_1 c_{234})\,l_4 + c_{23} l_3 + c_2 l_2)] \tag{A-15}
$$

$$
{}^{T_5}_{21}J = \left(-o_x P_y + o_y P_x\right) = c_1 s_{234} P_y - s_1 s_{234} p_x \tag{A-16}
$$

$$
{}^{T_5}_{31}J = \left(-a_x P_y + a_y P_x\right) = -s_1 P_y - c_1 P_x \tag{A-17}
$$

$$
{}^{T_5}_{41}J = s_{234} \tag{A-18}
$$

$$
J_{21} = 0 \tag{A-19}
$$

$$
J_{22} = 0 \tag{A-20}
$$

$$
J_{32} = -c_{23}\,(c_4 l_4 + l_3 + s_{23} s_4 l_4 + c_2 l_2) \tag{A-21}
$$

$$
J_{42} = -s_{23} c_4 - s_4 c_{23}) \tag{A-22}
$$

$$
J_{13} = [(-c_{34} c_3\,(c_4 l_4 + l_3) - s_3 s_4 l_4 + l_2) + s_{34}\,(c_3 c_4 l_4 + l_3) - s_3 s_4 l_4 + l_2)] \tag{A-23}
$$

$$
J_{23} = [s_{34} s_3\,(c_4 l_4 + l_3) + c_3 s_4 l_4 + c_{34}(c_3\,(c_4 l_4 + l_3) - s_3 s_4 l_4 + l_2] \tag{A-24}
$$

$$
J_{32} = 0 \tag{A-25}
$$

$$
J_{43} = 0 \tag{A-26}
$$

$$
J_{14} = [(-c_4)\,(s_4 l_4) + s_4(c_4 l_4 + l_3)] \tag{A-27}
$$

$$
J_{24} = [s_4\,(s_4 l_4) + c_4\,(c_4 l_4 + l_3)] \tag{A-28}
$$

$$
J_{34} = 0 \tag{A-29}
$$

$$
J_{44} = 0 \tag{A-30}
$$

ACKNOWLEDGMENT

(Taimoor Zahid and Zareena Kausar contributed equally to this work.)

REFERENCES

[1] D. Lee, T. Seo, and J. Kim, "Optimal design and workspace analysis of a mobile welding robot with a 3P3R serial manipulator," *Robot. Auto. Syst.*, vol. 59, no. 10, pp. 813–826, Oct. 2011, doi: 10.1016/j.robot.2011.06.004.

[2] B. Zi, H. Sun, Z. Zhu, and S. Qian, "The dynamics and sliding mode control of multiple cooperative welding robot manipulators," *Int. J. Adv. Robotic Syst.*, vol. 9, no. 2, pp. 1–10, 2012, doi: 10.5772/50641.

[3] J. E. Agapakis, J. M. Katz, J. M. Friedman, and G. N. Epstein, "Vision-aided robotic welding: An approach and a flexible implementation," *Int. J. Robot. Res.*, vol. 9, no. 5, pp. 17–34, Oct. 1990, doi: 10.1177/027836499000900502.

[4] J. N. Pires, A. Loureiro, T. Godinho, P. Ferreira, B. Fernando, and J. Morgado, "Welding robots," *IEEE Robot. Autom. Mag.*, vol. 10, no. 2, pp. 45–55, Jun. 2003, doi: 10.1109/MRA.2003.1213616.

[5] N. Tom, D. K. Badam, V. K. Singore, and V. L. K. Narayana, "Design and implementation of mobile robotic manipulator for welding using PLC," *Sens. Transducers*, vol. 188, no. 5, pp. 96–101, 2015.

[6] T. Zhang, M. Wu, Y. Zhao, X. Chen, and S. Chen, "Optimal motion planning of mobile welding robot based on multivariable broken line seams," *Int. J. Robot. Autom.*, vol. 29, no. 2, pp. 215–223, 2014, doi: 10.2316/Journal.206.2014.2.206-4032.

[7] T. Zhang, M. Wu, Y. Zhao, and S. Chen, "Motion planning for a new-model obstacle-crossing mobile welding robot," *Ind. Robot: Int. J.*, vol. 41, no. 1, pp. 87–97, Jan. 2014, doi: 10.1108/IR-05-2013-353.

[8] T. Zhang, S. Chen, M. Wu, Y. Zhao, and X. Chen, "Optimal motion planning of all position autonomous mobile welding robot system for fillet seams," *IEEE Trans. Autom. Sci. Eng.*, vol. 10, no. 4, pp. 1147–1151, Oct. 2013, doi: 10.1109/TASE.2013.2252462.

[9] T. Zhang and S.-B. Chen, "Optimal posture searching algorithm on mobile welding robot," *J. Shanghai Jiaotong Univ. (Sci.)*, vol. 19, no. 1, pp. 84–87, Feb. 2014, doi: 10.1007/s12204-014-1477-7.

[10] A. G. Dharmawan, B. W. C. Sedore, G. S. Soh, S. Foong, and K. Otto, "Robot base placement and kinematic evaluation of 6R serial manipulators to achieve collision-free welding of large intersecting cylindrical pipes," in *Proc. 39th Mech. Robot. Conf.*, Aug. 2015, Art. no. V05CT08A010, doi: 10.1115/DETC2015-47038.

[11] M. Dahari and J.-D. Tan, "Forward and inverse kinematics model for robotic welding process using KR-16KS KUKA robot," in *Proc. 4th Int. Conf. Modeling, Simulation Appl. Optim.*, Apr. 2011, pp. 1–6, doi: 10.1109/ICMSAO.2011.5775598.

[12] G. Meijuan, T. Jingwen, and L. Erhong, "Intelligent control system of welding Torch's attitude for pipeline welding robot," in *Proc. 8th Int. Conf. Electron. Meas. Instrum.*, Aug. 2007, pp. 3–665, doi: 10.1109/ICEMI.2007.4351005.

[13] A. R. D. Tipi and S. A. Mortazavi, "A new adaptive method (AF-PID) presentation with implementation in the automatic welding robot," in *Proc. IEEE/ASME Int. Conf. Mechtronic Embedded Syst. Appl.*, Oct. 2008, pp. 25–30, doi: 10.1109/MESA.2008.4735715.

[14] M. Young Kim, K.-W. Ko, H. Suck Cho, and J.-H. Kim, "Visual sensing and recognition of welding environment for intelligent shipyard welding robots," in *Proc. IEEE/RSJ Int. Conf. Intell. Robots Syst. (IROS)*, vol. 3, Oct./Nov. 2000, pp. 2159–2165, doi: 10.1109/IROS.2000.895290.

[15] Y. B. Jeon and S. B. Kim, "Modeling and motion control of mobile robot for lattice type welding," *KSME Int. J.*, vol. 16, no. 1, pp. 83–93, Jan. 2002, doi: 10.1007/BF03185158.

[16] B.-O. Kam, Y.-B. Jeon, and S.-B. Kim, "Motion control of two-wheeled welding mobile robot with seam tracking sensor," in *Proc. IEEE Int. Symp. Ind. Electron. (ISIE)*, vol. 2, Jun. 2001, pp. 851–856, doi: 10.1109/ISIE.2001.931579.

[17] T. L. Chung, T. H. Bui, T. T. Nguyen, and S. B. Kim, "Sliding mode control of two-wheeled welding mobile robot for tracking smooth curved welding path," *KSME Int. J.*, vol. 18, no. 7, pp. 1094–1106, Jul. 2004.

[18] Q. Tang, "Localization and tracking control for mobile welding robot," *Ind. Robot: Int. J.*, vol. 41, no. 3, pp. 259–265, May 2014, doi: 10.1108/IR-07-2013-377.

[19] G. Pan, E. Guan, F. Yang, A. Ren, and P. Gao, "Optimal motion planning for mobile welding robot," in *Proc. Int. Conf. Intell. Robot. Appl.*, 2017, pp. 124–134, doi: 10.1007/978-3-319-65292-4_12.

[20] T. D. Cuong and N. T. Phuong, "Adaptive sliding mode control of mobile manipulator welding system for horizontal fillet joints," *Am. J. Eng. Res. (AJER)*, vol. 9, pp. 124–138, Feb. 2015.

[21] C. F. Goh, K. Vazquez-Santiago, and K. Shimada, "Landing a mobile robot safely from tall walls using manipulator motion generated from reinforcement learning," in *Proc. IEEE 16th Int. Conf. Autom. Sci. Eng. (CASE)*, Aug. 2020, pp. 1578–1583, doi: 10.1109/CASE48305.2020.9216977.

[22] D. Zhang, Q. Zou, S. Guo, and H. Qu, "Kinematics and performances analysis of a novel hybrid welding robot," *Int. J. Robot. Autom.*, vol. 35, no. 4, Jan. 2020, doi: 10.2316/J.2020.206-0101.

[23] G. Wen, L. Xu, and F. He, "Offline kinematics simulation of 6-DOF welding robot," in *Proc. Int. Conf. Measuring Technol. Mechatronics Autom.*, Apr. 2009, pp. 283–286, doi: 10.1109/ICMTMA.2009.608.

[24] G. Yanfeng, Z. Hua, and Y. Yanhui, "Kinematical modeling of mobile welding robot for lattice type seam tracking," in *Proc. 2nd Int. Conf. Intell. Control Inf. Process.*, Jul. 2011, pp. 355–359, doi: 10.1109/ICICIP.2011.6008264.

[25] B. Maqueira, C. I. Umeagukwu, and J. Jarzynski, "Application of ultrasonic sensors to robotic seam tracking," *IEEE Trans. Robot. Autom.*, vol. 5, no. 3, pp. 337–344, Jun. 1989, doi: 10.1109/70.34769.

[26] B.-O. Kam, Y.-B. Jeon, and S.-B. Kim, "Motion control of two-wheeled welding mobile robot with seam tracking sensor," in *Proc. IEEE Int. Symp. Ind. Electron. (ISIE)*, vol. 2, Jun. 2001, pp. 851–856, doi: 10.1109/ISIE.2001.931579.

[27] N. Ku, J.-H. Cha, K.-Y. Lee, J. Kim, T.-W. Kim, S. Ha, and D. Lee, "Development of a mobile welding robot for double-hull structures in shipbuilding," *J. Mar. Sci. Technol.*, vol. 15, no. 4, pp. 374–385, Dec. 2010, doi: 10.1007/s00773-010-0099-5.

[28] M. D. Ngo, V. H. Duy, N. T. Phuong, S. B. Kim, and M. Oh, "Two-wheeled welding mobile robot for tracking a smooth curved welding path using adaptive sliding-mode control technique," *Int. J. Control, Automat., Syst.*, vol. 5, no. 3, pp. 283–294, 2007.

[29] Z. Bi, H. Wu, Y. He, P. Zhang, Y. Guan, and G. Liu, "Offline motion planning on spherical surfaces for a manipulator," in *Proc. IEEE Int. Conf. Robot. Biomimetics (ROBIO)*, Dec. 2014, pp. 1082–1087, doi: 10.1109/ROBIO.2014.7090476.

[30] F. A. Salem, "Kinematics and dynamic models and control for differential drive mobile robots," *Int. J. Current Eng. Technol*, vol. 3, pp. 253–263, Jan. 2013.

[31] G. Yanfeng, Z. Hua, M. Zhiwei, and P. Junfei, "Predictive fuzzy control for a mobile welding robot seam tracking," in *Proc. 7th World Congr. Intell. Control Autom.*, 2008, pp. 2271–2276, doi: 10.1109/WCICA.2008.4593276.

[32] M. D. Ngo, N. T. Phuong, V. H. Duy, H. K. Kim, and S. B. Kim, "Control of two wheeled welding mobile manipulator," *Int. J. Adv. Robotic Syst.*, vol. 4, no. 3, p. 32, Sep. 2007, doi: 10.5772/5685.

[33] T. Phuc Tran, T. Lam Chung, H. Kyeong Kim, S. Bong Kim, and M. Suk Oh, "Trajectory tracking of mobile manipulator for welding task using sliding mode control," in *Proc. 30th Annu. Conf. IEEE Ind. Electron. Soc. (IECON)*, vol. 1, Nov. 2004, pp. 407–412, doi: 10.1109/IECON.2004.1433345.

[34] R. Bostelman, "Performance measurement of mobile manipulators," Ph.D. dissertation, Dept. Comput. Sci., Univ. Burgundy, Dijon, France, 2018. [Online]. Available: https://tel.archives-ouvertes.fr/tel-01803721/document

[35] Z. Zhang, W. Ren, Z. Yang, and G. Wen, "Real-time seam defect identification for al alloys in robotic arc welding using optical spectroscopy and integrating learning," *Measurement*, vol. 156, May 2020, Art. no. 107546.

[36] M. F. Shah, Z. Kausar, and F. K. Durrani, "Design, modeling and simulation of six degree of freedom machining bed," *Proc. Pakistan Acadmey Sci.*, vol. 53, no. 2, pp. 163–176, 2016.

[37] M. F. Shah, Z. Kausar, and M. U. Farooq, "Kinematic modeling and analysis of a 6 DOF parallel machining bed," in *Proc. 22nd Int. Multitopic Conf. (INMIC)*, Nov. 2019, pp. 1–5, doi: 10.1109/INMIC48123.2019.9022802.

[38] P. C. Santos, R. C. S. Freire, E. A. N. Carvalho, L. Molina, and E. O. Freire, "M-FABRIK: A new inverse kinematics approach to mobile manipulator robots based on FABRIK," *IEEE Access*, vol. 8, pp. 208836–208849, 2020.

[39] J. Liao, F. Huang, Z. Chen, and B. Yao, "Optimization-based motion planning of mobile manipulator with high degree of kinematic redundancy," *Int. J. Intell. Robot. Appl.*, vol. 3, no. 2, pp. 115–130, Jun. 2019.

TAIMOOR ZAHID received the B.Sc. degree in electrical engineering from the University of Engineering and Technology, Taxila, Pakistan, in 2011, and the Ph.D. degree in computer applied technology from the University of Chinese Academy of Sciences, Beijing, China, in 2018.

He is currently working with the College of Mechatronics and Control Engineering, Shenzhen University, China. His research interests include robotics, state estimation and intelligent control for EV, and energy management systems.

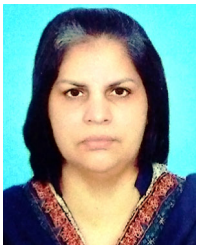

ZAREENA KAUSAR received the B.S. degree in mechanical engineering from UET Lahore, Pakistan, the M.S. degree in mechanical engineering from the National University of Ireland, the M.S. degree in mechatronics engineering from UET Lahore, and the Ph.D. degree from The University of Auckland, New Zealand. She worked as the Chair of the Department of Mechatronics Engineering, Air University, Islamabad. Her research interests include non-linear control systems, robotics, and bio-mechatronics.

MUHAMMAD FAIZAN SHAH received the B.E. degree in mechatronics engineering from Air University, Islamabad, in 2015, the master's degree in mechanical engineering from KFUEIT, R. Y. Khan, in 2020. He has been working as a Lab Engineer with the Department of Mechanical Engineering, KFUEIT, since April 2016. His research interests include to develop intelligent manufacturing systems, robotics, and control systems.

MUHAMMAD TALLAL SAEED received the B.Sc. and master's degrees in electrical engineering from the University of Engineering and Technology, Taxila, Pakistan, in 2011 and 2013, respectively, and the Ph.D. degree in control theory and control engineering from Beihang University, Beijing, China, in 2019.

He is currently working as an Assistant Professor with the Department of Mechatronics and Biomedical Engineering, Air University, Pakistan. His research interests include modeling and simulation, robotics, and control systems.

JIANFEI PAN (Member, IEEE) received the Ph.D. degree from the Department of Electrical Engineering, Hong Kong Polytechnic University, Hong Kong, in 2006.

He is currently working with the College of Mechatronics and Control Engineering, Shenzhen University. His research interests include motion control, actuator design, and robotics.